2022

A Comparison of IMPA2 & ISYNA1 Gene Expression and Intracelular Myo-Inositol Levels in Bipolar and Non-bipolar Disorder Derived Human Lymphoblasts

Christina Rosette
rosette@andrews.edu

ABSTRACT

A COMPARISON OF *IMPA2* & *ISYNA1* GENE EXPRESSION AND INTRACELLULAR *MYO-INOSITOL* LEVELS IN BIPOLAR AND NON-BIPOLAR DISORDER DERIVED HUMAN LYMPHOBLASTS

By

CHRISTINA ROSETTE

Chair: Marlene Murray, Ph.D.

ABSTRACT OF GRADUATE STUDENT RESEARCH
THESIS

Andrews University

College of Arts and Sciences

Title: A COMPARISON OF *IMPA2* & *ISYNA1* GENE EXPRESSION AND INTRACELLULAR *MYO*-INOSITOL LEVELS IN BIPOLAR AND NON-BIPOLAR DISORDER DERIVED HUMAN LYMPHOBLASTS

Name of Researcher: Christina Rosette

Name and Degree of Faculty Chair: Marlene Murray, Ph.D.

Date Completed: June 2022

The thesis objective was to determine if *myo*-inositol concentration levels and the gene expression of *IMPA2* & *ISYNA1* differ among bipolar disorder types 1 and 2 compared to healthy controls (non-bipolar disorder). Previous studies have correlated different *myo*-inositol concentration levels with specific phases of bipolar and pharmaceutical treatments. Two genes, inositol monophosphatase 2 (*IMPA2*) and inositol-3-phosphate synthase 1 (*ISYNA1*), involved in de novo *myo*-inositol biosynthesis have been implicated in the pathophysiology of bipolar. In this study, differences in *myo*-inositol concentration and *IMPA2* & *ISYNA1* gene expression in lymphoblasts derived from subjects with bipolar types 1, 2, and healthy control were measured spectrophotometrically and by RT-qPCR respectively. Myo-inositol concentration assay results showed statistically significant differences in *myo*-inositol concentration in bipolar type 1 compared to type 2 and non-bipolar disorder. The relative gene expression of *IMPA2* was twofold higher in both types of bipolar compared to healthy controls. The relative gene expression of *ISYNA1* was 0.47-fold higher in bipolar 1; and 0.76-fold higher in bipolar 2 compared to healthy control. This study found both *ISYNA1* and *IMPA2* expressed relatively higher in bipolar compared to non-bipolar; and bipolar type 1 had significantly higher concentrations of *myo*-inositol compared to type 2 and non-bipolar disorder.

Andrews University

College of Arts and Sciences

A COMPARISON OF *IMPA2* & *ISYNA1* GENE EXPRESSION AND INTRACELLULAR *MYO*-INOSITOL LEVELS IN BIPOLAR AND NON-BIPOLAR DISORDER DERIVED HUMAN LYMPHOBLASTS

A Thesis

Presented in Partial Fulfillment

of the Requirements for the Degree

Master of Science

by

Christina Rosette

June 2022

TABLE OF CONTENTS

LIST OF FIGURES

LIST OF ABBREVIATIONS

cAMP	cyclic AMP
cGMP	cyclic GMP
DAG	diacylglycerol
DSM IV	Diagnostics & Statistical Manual of Mental Health Disorders IV
ER	endoplasmic reticulum
GPCR	g-protein-coupled transmembrane receptors
IMPase 2	Inositol Monophosphatase 2
IMPA2	Inositol Monophosphatase 2
INT	iodonitrotetrazolium chloride
IP3	inositol-1, 4, 5-trisphosphate
ISYNA1	inositol-3-Phosphate Synthase 1
MIPS	*Myo*-inositol 1-phosphate synthase
MRI	Magnetic resonance imaging
NIGMS	National Institute of General Medical Sciences
PCR	polymerase chain reaction
PIP_2	phosphatidylinositol biphosphate
PKC	protein kinase C
PLC	phospholipase C
qPCR	quantitative polymerase chain reaction
RPMI	Roswell Park Memorial Institute
RT-qPCR	reverse transcription quantitative PCR
TBE	tris/borate/EDTA

ACKNOWLEDGMENTS

ACADEMIC SUPPORT

Thesis Committee: Dr. Murray, Dr. Smith, Dr. Lyons

The Andrews Biology Department Faculty & Administrative Staff

FINANCIAL SUPPORT

Graduate Student Grant in Aid of Research

Faculty Research Grant

Research Funding donated by Dr. Douglas & Dr. Elisabeth Wear

ADDITIONAL SUPPORT

Manuel & Vicki Rosette, Pamela Runge, Kathy Runge

Corriell Institute: Customer Service Reps

Andrews University Counseling & Testing Centers

Andrews University Student Success Center

CHAPTER 1: INTRODUCTION

Characterized by a high-energy manic phase and a low-energy depressive phase, bipolar disorder affects more than 45 million people globally. Bipolar is a complex multigenic disorder with an etiology that is still being defined (Ghadiri et al., 2016). For example, pharmaceutical therapies primarily used to treat bipolar are still being elucidated (Coyle and Duman, 2003). In theory, according to the *myo*-inositol depletion hypothesis, these drugs appear to work in part by decreasing the *myo*-inositol levels of the phosphatidyl-inositol (PI) signaling pathway (Harwood, 2004). This suggests individuals with bipolar may have higher concentrations of *myo*-inositol compared to a healthy neurotypical (or non-bipolar disorder). One possible reason for the increase in available *myo*-inositol could be the expression of mRNA for enzymes responsible for *myo*-inositol synthesis are upregulated in individuals with bipolar.

Shedding additional light on underlying genetic factors predisposing people to develop bipolar disorder may provide novel therapeutic targets. Current therapies have a range of efficacy, each laden with a variety of negative side effects such as nausea, diarrhea, excessive urination, cognitive impairment, and tremors (Stoll et al., 1999, Coyle and Duman, 2003). These may include Lithium, Valproate, and/or Carbamazepine, which are consistently used in the clinical setting, although their modes of action remain unclear. For that matter, details of bipolar pathophysiology itself are uncertain. Further study on bipolar-associated genes may provide a deeper understanding of bipolar pathophysiology and perhaps lead to the development of novel therapies with fewer negative side effects.

Bipolar is "a 'cyclic' or 'periodic' illness, with patients cycling 'up' into a manic or mixed-manic episode, then returning to normal, and cycling 'down' into a depressive episode from which

they likewise eventually more or less recover" (Association, 2000). Bipolar is characterized by extremes. For example, in her book "An Unquiet Mind: A Memoir of Moods & Madness," Kay Redfield Jamison, Professor of Psychiatry at Johns Hopkins University School of Medicine, described her experience with bipolar:

> *"When you're high it's tremendous. The ideas and feelings are fast and frequent like shooting stars, and you follow them until you find better and brighter ones. Shyness goes, the right words and gestures are suddenly there, the power to captivate others a felt certainty…Feelings of ease, intensity, power, well-being, financial omnipotence, and euphoria pervade one's marrow. But, somewhere, this changes. The fast ideas are far too fast, and there are far too many; overwhelming confusion replaces clarity. Memory goes. Humor and absorption on friends' faces are replaced by fear and concern. Everything previously moving with the grain is now against – you are irritable, angry, frightened, uncontrollable, and enmeshed totally in the blackest caves of the mind" – pg. 67 (Jamison 1995).*

While the manic phase may last several days or a couple of weeks, the depressive phase may last a few weeks or several months. A person may also experience going through rapid cycles of mania and depression. There are primarily three types of bipolar disorder: type 1, type 2, and cyclothymia (or cyclothymic disorder). Type 1 is characterized by a manic phase lasting for at least seven days (or severe enough to warrant a hospital admittance) along with a depressive episode lasting at least two weeks. Individuals with type 2 experience fewer extreme symptoms of mania (hypomania) and longer depressive episodes. Individuals with cyclothymia cycle through phases of hypomania and depression that are not as severe as type 1 and 2 (Goodwin and Jamison, 2007).

The symptoms associated with the highs (mania or hypomania) and lows (depression) of bipolar are evidence of changes in emotion regulation. These include learning, memory, cognitive control processes, executive function, and behavior. Previous studies have observed various abnormalities in volume, metabolism, and number of oligodendrocytes in between the prefrontal

cortex and limbic system of individuals with bipolar disorder (Mahon et al., 2010). Such differences have been observed specifically in the orbitofrontal cortex, dorsomedial prefrontal cortex, anterior cingulate cortex, and ventrolateral prefrontal cortex (Phillips et al., 2008). Similar differences have been found in regions within the limbic system including the limbic cortex, cingulate gyrus, striatum, parahippocampal gyrus, dentate gyrus, hippocampus, subicular complex, amygdala and hypothalamus ((Phillips et al., 2008, Mahon et al., 2010). These areas of the prefrontal cortex and limbic system work together in regulating emotions, making decisions, and cognitive processes through tracts of white matter connecting them.

A. Bipolar Disorder Pathophysiology

Previous studies have found damaged superficial white matter tracts connecting various parts of the prefrontal cortex with centers of the limbic system processing emotion in patients with bipolar disorder (Versace et al., 2008, Zhang et al., 2018) (Rajmohan and Mohandas, 2007). Such damage can be caused by modulations to intracellular communications in oligodendrocytes and/or neurons that make up these superficial white matter tracts. For example, the higher *myo*-inositol concentration the *myo*-inositol depletion hypothesis suggests changes in the phosphatidylinositol biphosphate signaling pathway (PIP_2) pathway may damage these superficial white matter tracks. The affected communication between these specific parts of the brain leads to disruptions in emotional regulation, executive functions, self-control, memory formation, etc. (Cendra et al., 2013).

Substantial evidence of structural differences including atrophy within the frontal lobe and increased incidence of signal hyperintensities on diffusion-weighted magnetic resonance imaging (MRI) in white matter tracks connecting the frontal lobe with the limbic system were found to be

more common in the brain of unipolar and bipolar depressed patients (Videbech, 1997). White matter lesions or damaged white matter appear as signal hyperintensities on MRI images. Damaged white matter can be detected using diffusion-weighted MRI, which uses fractional anisotropy to measure the restriction of diffusion of water molecules (Zhang et al., 2018). A fractional anisotropy value of 0 indicates unrestricted diffusion of water molecules in all directions and a value of 1 signals diffusion occurs along one axis and is fully restricted along other directions. This allows scientists to distinguish axons from surrounding tissue. Water molecules with fractional anisotropy values closer to 1 indicate regions where water is confined within cell membranes and can only diffuse along one axis. Within the brain, this occurs in axons. Whereas an area of water molecules with a fractional anisotropy value closer to 0 is not restricted by cell membranes. These reduced fractional anisotropy values have been associated with cerebrospinal fluid, local edema, changes in axonal morphologic structure and compromised myelin structure (Versace et al., 2008). One bipolar disorder study comparing the fractional anisotropy of white matter tracks connecting the prefrontal cortex and limbic system, found subjects with bipolar had aberrant fractional anisotropy, a significant negative correlation between age and fractional anisotropy, along with a significant negative correlation between medication load and fractional anisotropy (Versace et al., 2008). Another study found reduced fractional anisotropy in the superficial white matter in the bipolar patients compared to the healthy controls in various areas of the prefrontal cortex (Zhang et al., 2018).

One of the causes of reduced fractional anisotropy is aberrant myelin sheaths – a type of white matter damage (Phillips et al., 2008). The myelin sheaths of oligodendrocytes are the defining feature of white matter. By wrapping axons that connect neurons between regions of the prefrontal cortex and limbic system, oligodendrocytes provide protection from the surrounding extracellular environment. They also increase the speed of action potentials traveling down the axon by forcing the signal to “jump” between each myelin sheath. Damage to myelin sheaths of oligodendrocytes

can expose the axon, cause localized inflammation, and interfere with signal transduction down the axon. The evidence presented by the fractional anisotropy studies points to abnormal myelin sheaths (Phillips et al., 2008). Damaged myelin sheaths are the hallmark of multiple sclerosis, but are associated with brain cancers, spinal injury, major depressive disorder, and bipolar disorder (Mahon et al., 2010).

Glial reduction, signs of apoptosis, increased inflammation, decreased numerical density of grey matter, oligodendrocyte abnormalities, myelin pallor in the prefrontal cortex, anterior cingulate cortex and deep white matter have been associated with bipolar disorder (Mahon et al., 2010). One study found statistically significant lower myelin staining in major depressive disorder and bipolar depression compared to healthy control (Regenold et al., 2007). Disruptions to the cytoarchitecture of oligodendrocytes and neurons cause a fundamental alteration in cell resiliency and plasticity in these regions involved in emotion generation and regulation.

These previous studies support a hypothesis that oligodendrocyte myelin and neural axon cell damage localized to white matter connections between cognitive and emotional areas of the brain may be correlated with bipolar disorder (Mahon et al., 2010). The *myo*-inositol depletion hypothesis connects observations made on the modes of action of various bipolar therapies with observed anatomical differences in bipolar patients. Previous studies also reported observable differences in *myo*-inositol concentrations in the frontal lobes of people with bipolar, suicide victims and Major Depressive Disorder (Shimon et al., 1997). As *myo*-inositol is a precursor for the PIP_2 pathway, it provides a possible explanation (or at least a contributing factor) to the observed white matter lesions within the brain of individuals with bipolar.

i. Cellular-neurology pathophysiology

The PIP_2 cascade, in concert with other protein pathways, regulates cytoskeletal construction, Ca^{2+}cytosol levels, cell membrane integrity, apoptosis, ATP production, etc. Alterations of the PIP_2 cascade likely contribute to drastic changes in cell growth, morphology, function, and survival, as the cascade is integral to so many vital cell functions. If this occurs in developing neurons, it can stunt the progress of axon growth cones as neurons search for new synaptic connections. To that end, one study found lithium, VPA and carbamazepine blocked the collapse of sensory neuron growth cones and expanded the growth cone area. These effects were reversed when *myo*-inositol was added to the medium (Ohnishi et al., 2007a).

While alterations to the PIP_2 pathway are more likely to affect a neuron while it is growing than a mature neuron, the story is different for oligodendrocytes. A PIP_2 cascade glitch could cause any number of problems during the lifecycle of the oligodendrocyte, because of its involvement in cytoskeletal construction and influence on mitochondria (Streck et al., 2014). The function of oligodendrocytes is wrapped up in their ability to maintain healthy myelin sheaths (Regenold et al., 2007). If the myelin sheath degrades, signal propagation down the axon is directly affected (Mahon et al., 2010). The signal may take longer, get disconnected by the immune system's inflammatory response to myelin degradation, or be confused because areas along the axon are exposed to neurotransmitters in the surrounding extracellular matrix due to myelin degradation. By a wide range of means, the signal is affected (Zhang et al., 2018).

ii. PIP_2 pathway

Malfunctions of the PIP_2 pathway, vital to maintaining a healthy cell, can contribute to the development of white matter tract lesions between the cognitive and emotional centers of the brain.

The PIP_2 cascade is activated by G protein-coupled receptor (GPCR) that need to translate an extracellular signal to an intracellular signal.

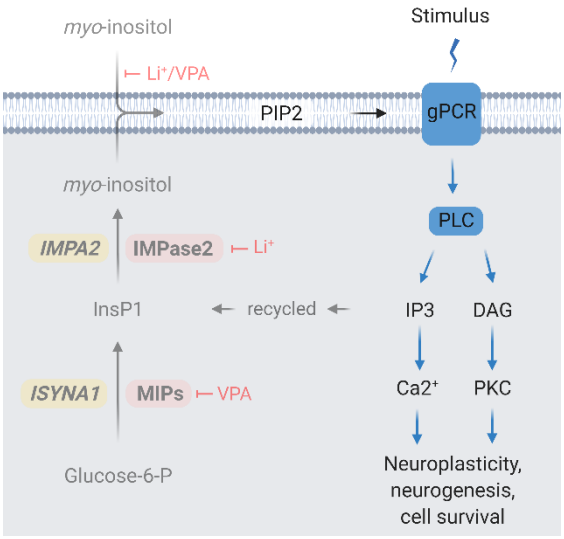

Figure 1. ***The PIP_2 Cascade****: Activated by certain GPCR receptors, the PIP_2 Cascade begins when PLC cleaves PIP_2 producing IP3 and DAG. IP3 signals the release of Calcium ions from the ER. DAG activates PKC. These second messengers regulate cytoskeletal construction, cytosol levels of Ca2+, cell membrane integrity, apoptosis, etc.(the myo-inositol synthetic pathway is pictured on the left) (made with biorender.com)*

When a GPCR linked to the phosphatidylinositol (PIP_2) system is activated by the appropriate ligand the alpha subunit (alpha q) dissociates from the GPCR complex and activates phospholipase C (PLC) which in turn hydrolyses phosphatidylinositol into inositol-1,4,5-trisphosphate (IP_3) and diacylglycerol (DAG). IP_3 activates IP_3 receptors in the endoplasmic reticulum membrane releasing Ca^{2+} into the cytosol from the endoplasmic reticulum.

Released $Ca^{2+}$from the endoplasmic reticulum is a 2nd messenger participating in several pathways as well. Ca^{2+} ions can activate caspase-mediated apoptosis, activate Ca^{2+} dependent proteins, and increase mitochondria membrane permeability. Consequently, releasing reactive oxygen species, reducing mitochondrial ATP synthesis, modulating cytoskeletal construction and/or cell membrane integrity. Increased intracellular Ca^{2+} has been described in bipolar disorder

(Machado-Vieira et al., 2009). Treatment with Li+ increases Bcl-2, a neuroprotective protein that downregulates endoplasmic reticulum calcium release (Machado-Vieira et al., 2009).

DAG activates protein kinase C (PKC) enzymes (Bronson and Konradi, 2010). PKC enzymes are kinases which phosphorylate other proteins, and therefore are integral to several intracellular pathways. PKC family enzymes modulate neuronal development, excitability, death, and consequently learning and memory. This is because PKC enzymes are involved in most neuronal processes such as neurotransmitter release and uptake, cytoskeletal construction, cell membrane integrity, regulating gene expression, and receptor and ion channel function (Bronson and Konradi, 2010).

B. *Myo*-inositol Depletion Hypothesis

The availability of the PIP_2 precursor, *myo*-inositol, influences how active the PIP_2 pathway can be. Several studies have begun to create a picture of the PIP_2 pathway's role in maintaining cell homeostasis . Previous studies have provided evidence to support that Lithium and VPA can affect how much *myo*-inositol is available to the cell (Ohnishi et al., 2007a, Dixon and Hokin, 1997, Coyle and Duman, 2003). According to the *myo*-inositol depletion hypothesis, Lithium and VPA depletion of intracellular *myo*-inositol reduces symptoms of mania (Harwood, 2004).

Previous studies have supported the *myo*-inositol depletion hypothesis in that the amount of available *myo*-inositol may be correlated with symptoms and treatment of bipolar disorder (Chengappa et al., 2000). In an animal model study, treatment with Lithium lowered intracellular *myo*-inositol concentration by 30% in rat cerebral cortex (Harwood, 2004). The preferred therapies, Lithium and VPA reduce symptoms of the manic phase, and lower intracellular *myo*-inositol levels. (Machado-Vieira et al., 2009); (Coyle and Duman, 2003).

i. *Myo*-inositol Biosynthesis

Myo-inositol is a precursor of the membrane phospholipid, phosphatidylinositol (PI), and its phosphorylated derivatives phosphatidylinositol phosphates (PIP) (Ohnishi et al., 2007a). The cell has 3 sources of *myo*-inositol: it can snag some floating by in the extracellular space, it can synthesize some de novo from glucose-6-phosphate, or it can recycle the 2nd messenger IP3 back into *myo*-inositol (Figure 2).

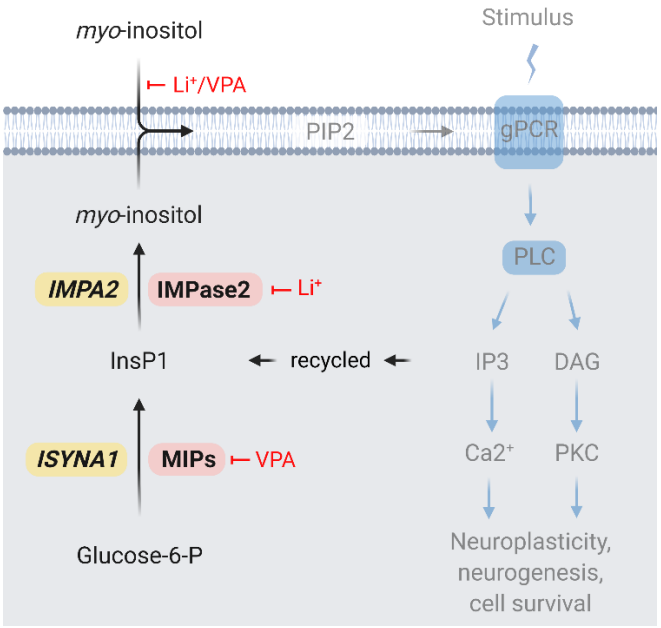

*Figure 2: **Sources of Myo-inositol**: The cell has three sources of myo-inositol: De novo synthesis, recycling from IP3, and extracellular capture. The Enzyme MIPs (ISYNA1) converts Glucose-6-phosphate to InsP1, beginning de novo synthesis. The Enzyme IMPase2 (IMPA2) begins the conversion of new and recycled InsP1 to myo-inositol. (made with biorender.com)*

The de novo synthesis of *myo*-inositol begins as the enzyme *myo*-inositol 1-Phosphate Synthase (MIPS) converts glucose-6-phosphate to *myo*-inositol 1 phosphate (InsP1) (Stoll et al., 1999). The cell can also recycle the 2nd messenger inositol (1,4,5) triphosphate (IP3) back into

InsP1. The enzymes *myo*-inositol monophosphatase 1 & 2 (IMPase1 & IMPase2) then catalyze the dephosphorylation of InsP1 to *myo*-inositol (Coyle and Duman, 2003) (Figure 2).

Out of the genes involved in the synthesis of *myo*-inositol, the genes coding for MIPs (*ISYNA1*) and IMPase2 (*IMPA2*) were selected for this study (Coyle and Duman, 2003, Stoll et al., 1999). Previous studies provide evidence Lithium and VPA interact with these proteins. The resulting changing concentrations of *myo*-inositol may correlate with observed differences: include single nucleotide polymorphisms, location within a bipolar susceptibility locus on chromosome 18, in each gene (Dimitrova et al., 2005); (Agam et al., 2009). There may be genetic variation in these genes in people with bipolar disorder.

The homolog to *ISYNA1* in yeast (INO1) is commonly used to study the function of *ISYNA1*. The transcription of INO1 is regulated by extracellular *myo*-inositol levels, when levels are high transcription of INO1 is repressed (Yu et al., 2017). In one study using yeast as a model organism, human MIPs (isolated from post-mortem brain tissue) synthesis activity was reduced by 35%, while intracellular *myo*-inositol concentration was reduced by 25% in cells grown in therapeutically relevant concentrations of VPA (0.6mM) (Ju et al., 2004). MIPs requires a metal ion, typically Mg2+, as a coenzyme. Lithium noncompetitively inhibits the activity of MIPS by displacing Mg2+ (York et al., 1995).

Two single nucleotide polymorphisms (SNP) in the *IMPA2* promoter sequence were found preferentially transmitted to affected offspring (Sjøholt et al., 2000). One study correlated specific *IMPA2* SNPs unique to better Lithium treatment responders than non-responders, even though there was not a significant difference specific to bipolar disorder(Dimitrova et al., 2005). One study tested specific SNPs of *IMPA2* in individuals with bipolar disorder and found the patients who had the SNPs benefited more from Lithium treatment than other bipolar individuals(Sjøholt et al., 2000). Lithium proposed mechanism of action is noncompetitive inhibition of the enzyme IMPase which recycles *myo*-inositol (Coyle and Duman, 2003); (Machado-Vieira et al., 2009). Lithium

inhibits IMPase under therapeutic concentrations (~1 mM) (Ohnishi et al., 2007a). *IMPA2* is located within a susceptibility locus for bipolar on chromosome 18p11.2 (Dimitrova et al., 2005). MIPs and IMPase2 are of interest because not only do they make *myo*-inositol, but they also interact with Lithium and VPA. Even more interesting is how each interacts because each gene seems to act differently with each drug. This suggests that genetic mutations in *ISYNA1* & *IMPA2* may be contributing subtly to the development of bipolar and may also influence the efficacy of VPA treatments.

The hypothesis of this study was bipolar patients express *IMPA2* & *ISYNA1* differently and have different *myo*-inositol concentration levels as compared to neurotypical. This study did not take into consideration possible causes for differences in gene expression and *myo*-inositol. The difference between cyclothymia and the other two types of bipolar disorder is the shorter cycles and was not evaluated in this study. This study aims to provide evidence of existing differences, correlated with bipolar disorder types one and two, worth studying in more detail to better understand the pathophysiology of bipolar.

CHAPTER 2: METHODS

A. Cell Culture

This study was conducted using three immortalized lymphoblasts cell lines (LCLs) obtained from the National Institute of General Medical Sciences (NIGMS) Human Genetic Cell Repository at the Coriell Institute for Medical Research. These included bipolar 1 cells (GM07263), bipolar 2 cells (GM05236, later replaced by GM04952) and cells from an individual not diagnosed with bipolar (GM06138).

Each of the three lymphoblast cell lines were maintained according to NIGMS guidelines. Cell lines were incubated at 37° C and 5% CO2, suspended in 10 – 20ml of growth media. The RPMI 1640 growth media was supplemented with 1% pen-strep, 1% Glutamax, and 15% FBS. During each passage, cell culture flasks were inspected visually for contamination and cell viability densities were calculated via a hemocytometer. Each hemocytometer count was prepared as follows: 10ul of cell culture was diluted with 10ul Trypan Blue.

Cell flasks were passaged every two to five days to maintain a live cell concentration between 200,000 viable cells/ml - and 500,000 viable cells/ml. non-viable cell densities were not considered in downstream cell density calculations. Cells were stored long-term in liquid nitrogen. To prepare cells for storage, 5,000,000 live cells were pelleted via centrifugation at 100 xg for 10 minutes at 4-10°C, resuspended in freezing media (RPMI 1640, 30% FBS, 5% DMSO), then frozen overnight in an isopropanol bath before being transferred to long-term storage.

B. *Myo*-inositol Concentration Assay

Quantifying differences in *myo*-inositol concentration between the bipolar type 1, type 2, and non-bipolar cell lines was another aim of this study. To that end, an initial attempt to measure intracellular *myo*-inositol concentration was conducted using the PicoProbe fluorometric assay. This approach was eventually replaced by the more cost-effective and efficient spectrophotometric assay by Megazyme.

i. Fluorometric Assay

This assay indirectly quantifies the amount of *myo*-inositol by measuring a fluorescent product resulting from a two-step reaction. The *myo*-inositol concentration in each reaction is then determined from a *myo*-inositol concentration standard curve.

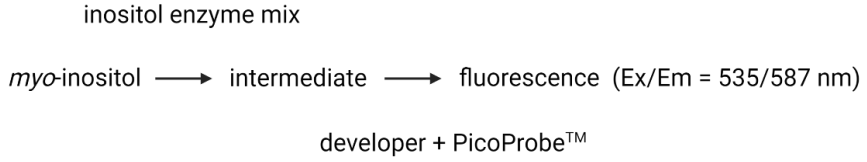

The standard curve was generated using varying concentrations from 0-500pmol: 0, 100, 200, 300, 400, and 500pmol of *myo*-inositol. The assay was conducted in duplicates using 96 well plates. Since the concentration of *myo*-inositol in each sample is determined from the *myo*-inositol standard curve, before conducting sample trials, the *myo*-inositol standard curve first needed to be generated. To each well was added: 50µl of a specific concentration of *myo*-inositol (diluted in assay buffer), 43µl kit assay buffer, 2µl kit enzyme mix, 2µl kit developer, 3µl and PicoProbe™ (in DMSO). After a 30-minute incubation at 37°C, the plate is loaded into the spectrofluorometer

and the fluorescence within each well of the plate was measured at Excitation = 535 nm and Emission = 545/650 nm; with a 10nm excitation slit and 5nm emission slit; using Cary Eclipse software and spectrofluorometer. To generate the standard curve, the 0 *myo*-inositol reading is subtracted from each *myo*-inositol standard reading. The corrected RFU (relative fluorescence unit) (isolated sample reading) is then applied to the *myo*-inositol standard curve to get nmol *myo*-inositol in the well. The range of emissions was expanded to include more wavelengths of light. This was done to document at what wavelength the fluorescent signal was strongest. Fluorescent signals were reported at 587nm.

ii. Spectrophotometry

The *myo*-inositol enzyme assay, Megazyme, was more efficient than the PicoProbe fluorometric assay and therefore was used to generate the reported sample *myo*-inositol data. The *myo*-inositol enzyme assay is based on two enzyme-facilitated reactions. *Myo*-inositol dehydrogenase oxidizes *myo*-inositol using the enzyme cofactor NAD+ producing 2,4,6/3,5-pentahydroxycyclohexanone, NADH , and H+. In the second reaction, catalyzed by diaphorase, NADH reduces iodonitrotetrazolium chloride (INT) to an INT-formazan product. The amount of INT-formazan, determined by the increase of absorbance at 492nm, is stoichiometric with the amount of *myo*-inositol.

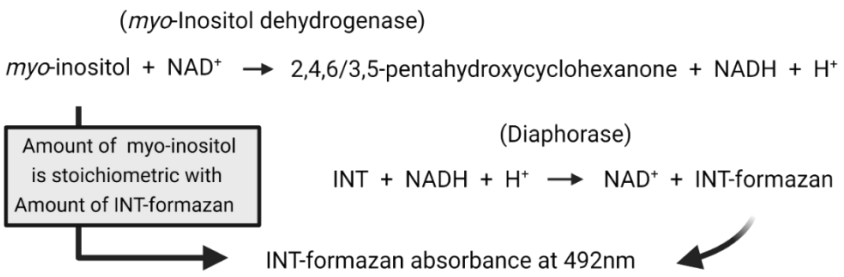

The samples were derived from homogenized cell pellets normalized by weight. For two of the three replicates 14ml cell culture was collected from each cell line. For one of the three replicates, 10ml cell culture was collected from each cell line. Cells from each cell line were spun at the highest speed in 50mL tubes for 15 minutes at ambient temperature. The supernatant was disposed of and 5mL distilled water was added to each cell pellet. After rinsing the cells via vortex, the cells were spun a second time at the highest speed for 15 minutes at ambient temperature. Without disturbing the pellet, the supernatant was discarded, and each cell pellet was weighed. Cell sample concentrations were normalized by weight. To determine the cell pellet weight, the weight of the empty 50mL tube was subtracted from the total weight of the cell pellet in the tube. Cell pellets were used immediately downstream or were stored at -20°C. Cell extracts were prepared by resuspending each cell pellet with 5mL distilled water. Each resuspended pellet was mixed by vortex. Each cell sample was then sonicated to lyse the cells. Then 1mL of the lysed homogenized cell sample was centrifuged at 13,000g for three minutes. 100µl of the extract was used per reaction.

To prepare the time-sensitive assay, the reactants for each reaction were prepared in disposable 1 cm light path cuvettes. Each assay had a blank cuvette prepared along with the various sample cuvettes. Each cell line was represented by one sample reaction cuvette. Each cuvette received 500µl distilled water, 100µl pH7.4 kit buffer, 20µl hexokinase (which removes any glucose present), 100µl sample, and 100µl reconstituted ATP. Each cuvette was covered with parafilm, mixed gently, and allowed to incubate at ambient temperature for 15 minutes. The blank cuvette contained no cell extract.

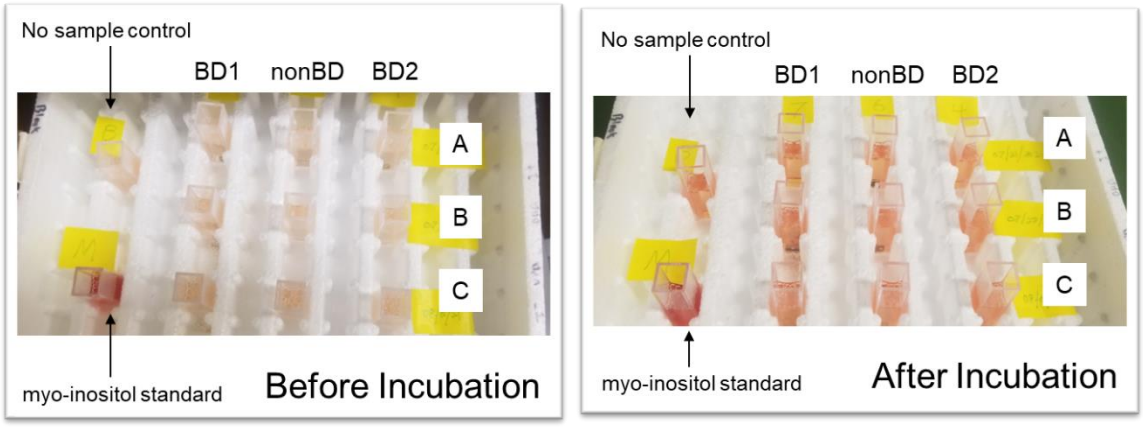

Figure 3. ***Spectrophotometric Assay Layout****: A negative and positive control cuvette were measured alongside the myo-inositol assay reaction cuvettes. (n=3) The formazan color shift in the reaction cuvettes before and after absorbance readings is visible to the naked eye.*

After incubating at ambient temperature for 15 minutes, each cuvette received 1ml pH 9.5 kit buffer, 20µl diaphorase suspension, and 500µl (light-sensitive) kit NAD+/INT. Each cuvette was mixed gently, protected from light until reading, and the absorbance (A_1) was recorded at 492 nm after approximately three minutes. After recording the absorbance (A_1) of every cuvette, 20µl *myo*-inositol dehydrogenase suspension was added to each cuvette to start the reaction. After gently mixing each cuvette, the cuvettes were protected from light and incubated for about 15 minutes at ambient temperature. The absorbance (A_2) was recorded for each cuvette in the same order as before. The recorded absorbance values and weight of the cell pellet for each cell line were used to calculate the concentration of *myo*-inositol in each sample.

The amount of INT-formazan, determined by the increase of absorbance at 492nm, is stoichiometric with the amount of *myo*-inositol. The increase in INT-formazan absorbance (ΔA) was calculated by subtracting (A_1) from (A_2) for each cuvette. The ΔA of *myo*-inositol was found by subtracting the blank ΔA from the sample ΔA. The ΔA of *myo*-inositol was then used to calculate the concentration of *myo*-inositol.

$$C\ \textit{myo}\text{-inositol} = \frac{V \times MW}{\varepsilon \times d \times v} \times \Delta A_{inositol}\ [g/L]$$

$$C = \frac{2.26 \times 180.16}{19900 \times 1.0 \times 0.1} \times \Delta A_{inositol}\ [g/L]$$

$$C = 0.2046 \times \Delta A_{inositol}\ [g/L]$$

V = final volume [mL]
MW = molecular weight of *myo*-inositol [g/mol]
ε = extinction coefficient of INT-formazan at 492 nm
(ε = 19900 [L x mol^{-1} x cm^{-1}])
d = light path [cm]
v = sample volume [mL]

Once the concentration of *myo*-inositol in each sample cuvette was determined using the equations provided by Megazyme, it was used to find the content of *myo*-inositol in each sample. The concentration of *myo*-inositol was normalized by weight using the content of *myo*-inositol formula: The content of *myo*-inositol (mg myo-inositiol/g total cells) was calculated by dividing *myo*-inositol concentration by total cells weight, using the following formula:

$$\text{Content of } \textit{myo}\text{-inositol} = \frac{C_{inositol}\ [g/L\ sample\ solution]}{weight_{sample}\ [g/L\ sample\ solution]}$$

C.Gene Expression Assay

i. mRNA Extraction & Quantification

The RNA in each sample pellet was extracted using Bio-Rad's Aurum Total RNA Mini Kit. To prepare cell samples, 2 million live cells from each cell line were pelleted by centrifugation at 12,5000g at ambient temperature for two minutes to collect cells from multiple cell culture flasks. The cell pellet was centrifuged twice. The supernatant was discarded, and the pellet was resuspended in 250 µl PBS and was either stored in the freezer at -20°C or used immediately for RNA extraction. According to the Bio-Rad Total RNA min Kit Spin Protocol, each subsequent centrifugation was done at 12,500g at ambient temperature. The sample pellets were centrifuged, and the supernatant discarded. The cells were lysed and homogenized with 350µl lysis (supplemented with 1% guanidine thiocyanate in β-mercaptoethanol) solution. 70% ethanol was added to the cell lysate and the cell lysate was filtered through an RNA binding column by centrifugation for one minute. The filtrate was discarded, and the column washed with 700µl low stringency wash via centrifuging for one minute. To remove genomic DNA, the column was incubated at ambient temperature with 80µl DNase (RNase free DNase reconstituted in 250 µl 10 mM Tris, pH 7.5) for 20 minutes. The column was then washed first with 700µl high stringency (guanidinium chloride) buffer by centrifugation for one minute, then 700µl low stringency buffer by centrifugation for one minute. This was followed by an additional centrifugation for two minutes to remove the residual wash solution. The column was transferred to capped microcentrifuge tubes and treated with 80µl elution solution for one minute at ambient temperature. The column was then centrifuged for two minutes to elute the total RNA. The RNA elutes for each cell line sample were used immediately or stored at -80°C. The mRNA concentration was determined using UV spectroscopy. Each eluant was diluted with nuclease-free water and absorbance was measured at

260nm. The absorbance values were multiplied by the dilution factor (3.3) and the RNA standard of 40µg/ml to determine RNA concentrations.

ii. cDNA Synthesis

The eluted RNA was reverse transcribed using Bio-Rad's iScript Reverse Transcription Supermix for RT-qPCR kit. A 96-well assay plate was prepared, on ice, for reverse transcription as follows: a reverse transcriptase (RT) reaction and no-RT reaction for each sample elute. Each 20µl reaction received nuclease-free water, mRNA elute, and either 4µl RT supermix or no-RT supermix. The amount of mRNA elute (and nuclease free water) in each reaction was based on RNA concentration and qPCR template calculations. The sealed plate was placed in a Bio-Rad RT quantitative thermocycler and cDNA was synthesized using the following protocol: priming for five minutes at 25°C, Reverse transcription for 20-minute 46°C, RT inactivation for one minute at 95°C. After reverse transcription the cDNA was used immediately or stored at -20°C for future use.

iii. Quantitative PCR

The relative gene expression of *IMPA2* & *ISYNA1* in bipolar 1 and 2 was measured using the Bio-Rad SYBR Green PCR system: commercially available PrimePCR™ SYBR® Green Primer assays (primers), PrimePCR™ SYBR® Green assays (commercial templates), SsoAdvanced Universal™ Supermix, and nuclease-free water. For each qPCR assay, a 96 well assay plate was prepared to amplify each GOI from each of the three cell lines along with the following controls. For each SYBR Green reaction with RT sample product, a corresponding SYBR

Green reaction with noRT sample product was included as a negative control. Each qPCR assay included reactions with commercial templates for each primer as a positive control and reactions without templates as a negative control. Each qPCR assay also included supermix and nuclease-free water reactions, and nuclease-free water only reactions contamination controls. Each step of the workflow included controls for genomic DNA contamination. Each RNA elute was incubated and rinsed with DNase before reverse transcription. To detect genomic DNA, each qPCR assay included a Bio-Rad designed DNA contamination control assay (gDNA) primer that amplifies non-coding DNA. The gDNA assay C_T values were used to compare relative levels of gDNA contamination present in different samples to determine if the qPCR assay results may be affected.

For each SYBR Green qPCR assay, the reaction wells of the 96 well plate were prepared, on ice, as follows: nuclease-free water (volume based on template volume), 10µl SsoAdvanced Universal Supermix, 1µl primer, and appropriate volume of (commercial or sample) template was added to each well. The volume of template added to each reaction was calculated from RNA concentration and qPCR calculations. The qPCR assay was conducted using the following protocol: after two minutes at 95°C for template denaturation, the temperature was raised from 65°C to 95°C in 5°C increments for five seconds, and the melting points were recorded. Immediately thereafter, 40 PCR cycles were performed by repeating the following thermocycling profile: denaturation at 95°C for five seconds, then annealing and extension at 62°C for 30 seconds. At the end of the PCR amplification, a second melt curve was obtained, the temperature was raised from 65°C to 95°C in 5°C increments for five seconds, and the melting points were recorded. After completing the PCR amplification, the 96 well PCR plate was stored at -20°C for use in gel electrophoresis. To visualize the qPCR assay product lengths, samples from the qPCR amplicon were run on a 5% agarose gel containing 0.006% ethidium bromide, using Tris/Borate/EDTA (TBE) as the running buffer. The Ultra-Low Range DNA Ladder (Invitrogen) was used to determine product length in base pairs. The DNA was electrophoresed at 100V for 30 minutes and imaged under UV light.

iv. Relative Gene Expression Determination

Relative gene expression of *ISYNA1* & *IMPA2* was determined using the amplification curve C_T values by the $\Delta\Delta$ C_T calculation method. Also known as the Livak method, it is used to determine the relative difference in the expression level of a target gene in test samples compared to a calibrator sample. The non-bipolar samples served as the calibrator to measure relative gene expression in bipolar 1 and 2 samples. The $\Delta\Delta$ C_T assumes that both target and reference genes are amplified with efficiencies near 100% and within 5% of each other. The percent efficiency of the PrimePCR SYBR Green assay primers are as follows: *ISYNA1* = 99%, *IMPA2* = 96%, and ACTG1 = 99% (Bio-Rad). Using the $\Delta\Delta$ C_T method, first, the relative difference in C_T was calculated between each GOI - *ISYNA1* & *IMPA2* - and the average expression of the reference gene - *ACTG1*. This Δ C_T for each gene was then used to calculate $\Delta\Delta$ C_T (for bipolar 1 and 2) using the non-bipolar samples as the calibrator.

$$\Delta C_T = C_{T\,(GOI)} - C_{T\,(refrence)}$$

$$\Delta\Delta C_T = \Delta C_{T\,(test)} - \Delta C_{T\,(calibrator)}$$

$$2^{-\Delta\Delta C_T} = \text{normalized expression (GOI)}$$

CHAPTER 3: RESULTS

For this study, a *myo*-inositol concentration assay was used to measure intracellular *myo*-inositol. In addition, Real-Time quantitative PCR (RT-qPCR) was done to measure relative IMPA2 & ISYNA1 gene expression. Both assays were done using immortalized lymphoblast cell lines initially derived from three different individuals: an individual with bipolar type 1, one with type 2, and a non-bipolar (healthy control). Lymphoblasts were chosen as the model since several previous studies have already used them and the cell lines tend to be more robust in cell culture (Milanesi et al., 2017); (Walss-Bass and Fries, 2018); (Fries et al., 2017). *Myo*-inositol concentrations within the same three cell lines were measured using a *myo*-inositol assay kit. For each experiment, the mean from multiple assay replicates was used to represent the results for relative gene expression and *myo*-inositol concentration respectively.

A. *Myo*-inositol Concentration

i. Fluorometric Assay

For the fluorometric assay, the *myo*-inositol concentration in each reaction is determined from a *myo*-inositol concentration standard curve. Initial standard curve generation trials produced inconsistent data. The assay methodology finally produced a standard curve (in triplicate) after a few optimization (5) trials. Due to the extensive optimization involved in the fluorometric assay, the spectrophotometric assay was used instead.

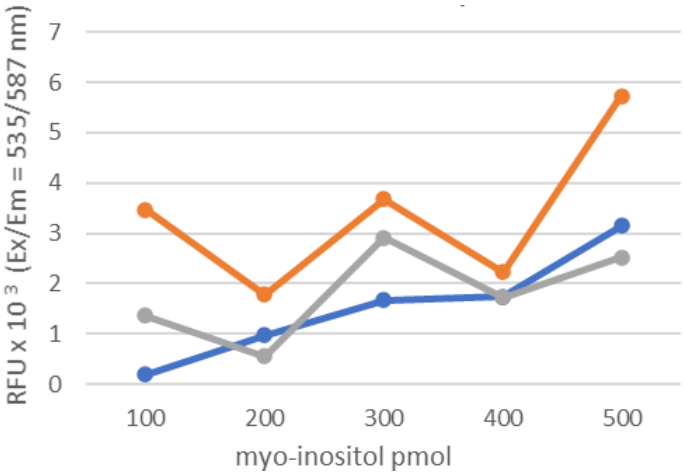

Figure 4: ***Myo-inositol Standard Curve Initial Trial****: Standard Curve of myo-inositol (n=3).*

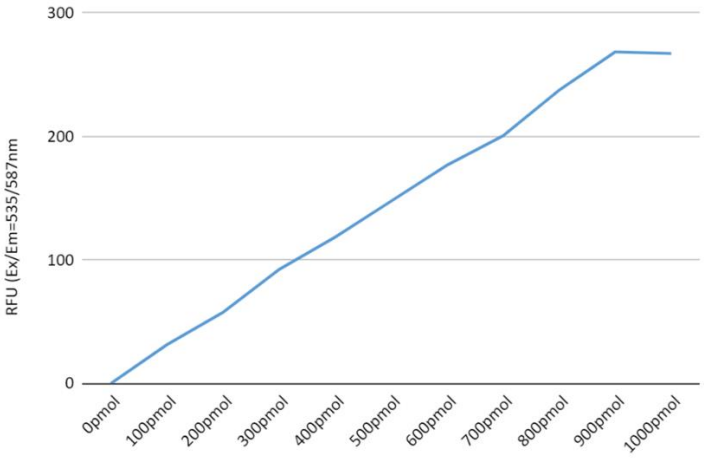

Figure 5: ***Myo-inositol Standard Curve Fifth Trial****: Standard Curve (n=3)*

ii. Spectrophotometric Assay

The average *myo*-inositol concentration from bipolar type 1, type 2, and non-bipolar did show a statistically significant difference. While *myo*-inositol concentrations were similar between bipolar 2 and non-bipolar samples (1.8 and 1.7 *myo*-inositol g/l / sample g/l

respectively); the concentration of *myo*-inositol in the bipolar 1 sample (4.7 *myo*-inositol g/l / sample g/l) was almost three times as high ($F = 12.5$, $p < 0.05$). On average, the bipolar 1 sample had a higher concentration of *myo*-inositol than bipolar 2 or non-bipolar samples.

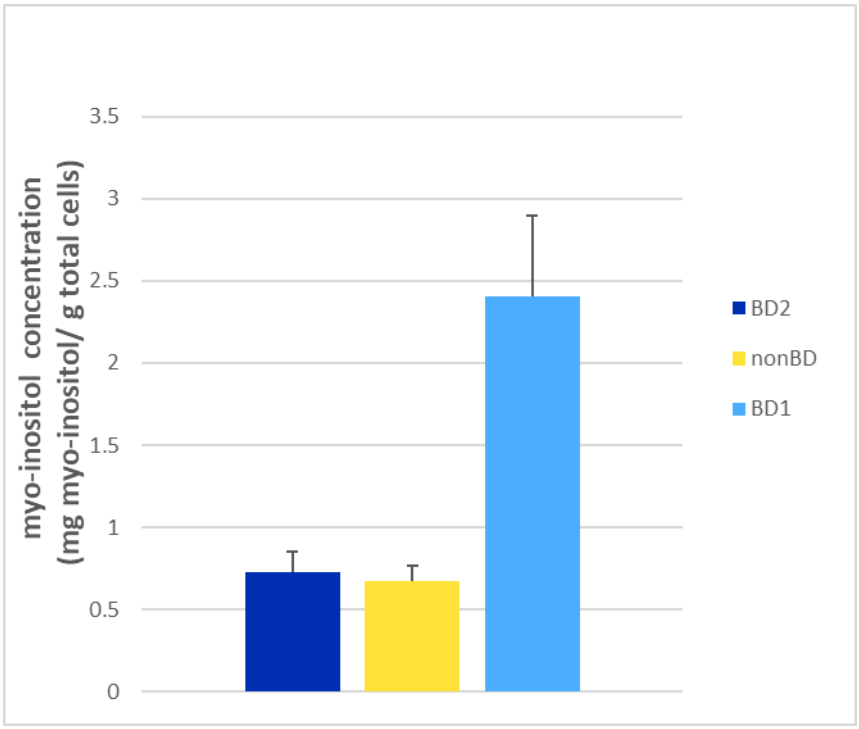

Figure 6: ***Mean myo-inositol concentration****: in bipolar type 1, type 2, and non-bipolar cell extracts, n= 3 ($F = 12.5$, $p < 0.05$ by ANOVA).*

B. Relative Gene Expression

Measuring the relative gene expression differences of *IMPA2* & *ISYNA1*, between the bipolar type 1, type 2, and non-bipolar cell lines was another aim of this study. The two genes of interest (GOI), *IMPA2* & *ISYNA1*, code for enzymes that are responsible for catalyzing specific steps within the *myo*-inositol biosynthesis pathway. They interact with Lithium and VPA in unique

ways. Previous studies have documented differences in each correlated with bipolar. Detecting whether either is expressed differently in bipolar provides further information on the pathophysiology of bipolar disorder. Relative *IMPA2* & *ISYNA1* gene expression was determined by quantitative PCR using RNA extracted from the three cell lines.

Figure 7 shows the relative gene expression of *ISYNA1* mRNA by RT-qPCR. Relative *ISYNA1* expression in the bipolar 2 cells was 0.47-fold higher than the non-bipolar control. Relative *ISYNA1* expression in the bipolar 1 cells was 0.76-fold higher than the non-bipolar control.

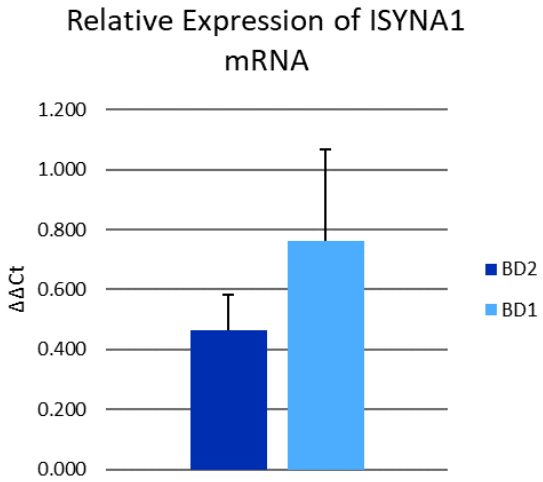

Figure 7:ISYNA1 gene expression in bipolar type 1 and type 2 relative to non-bipolar, n=3.

.

Figure 8 shows the amplification curves of *ACTG1* RT, *ISYNA1* RT, and gDNA RT RT-qPCR reactions in triplicate. *ISYNA1* cDNA had C_T values ranging between 20 and 22 across bipolar type 1, type 2, and non-bipolar cell lines as expected. The reference gene *ACTG1* had C_T values between 13 and 15 across type 1 and 2, and non-bipolar cell lines as expected. The C_T values for the gDNA contamination assay were > 31 and therefore considered negligible.

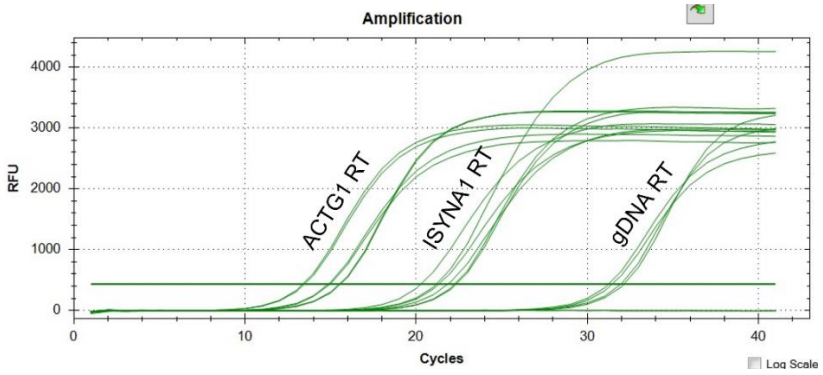

*Figure 8**: Amplification Curves**: ACTG1, ISYNA1 and gDNA RT-qPCR reaction wells show the thresh hold cycle (Ct) for each primer assay*

Figure 9 shows the relative gene expression of *IMPA2* mRNA by RT-qPCR. Relative *IMPA2* expression in the bipolar type 2 cells was 2-fold higher than non-bipolar *IMPA2* expression, and bipolar type 1 lymphoblasts had 2.1-fold higher *IMPA2* expression compared to the non-bipolar control.

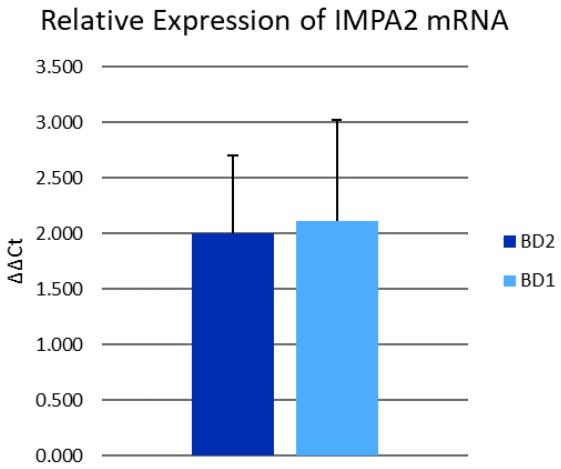

Figure 9: IMPA2 gene expression in bipolar 1 and bipolar 2 disorder relative to non-bipolar disorder, n=3.

Figure 10 shows the amplification curves of *ACTG1* RT, *IMPA2* RT, and gDNA RT RT-qPCR reactions in triplicate. *IMPA2* cDNA had C_T values ranging between 21 and 28 across bipolar type 1, type 2 and non-bipolar cell lines. The reference gene *ACTG1* had C_T values between 13 and 15 across bipolar type 1, type 2, and non-bipolar cell lines. The C_T values for the gDNA contamination assay were > 31 and therefore considered negligible.

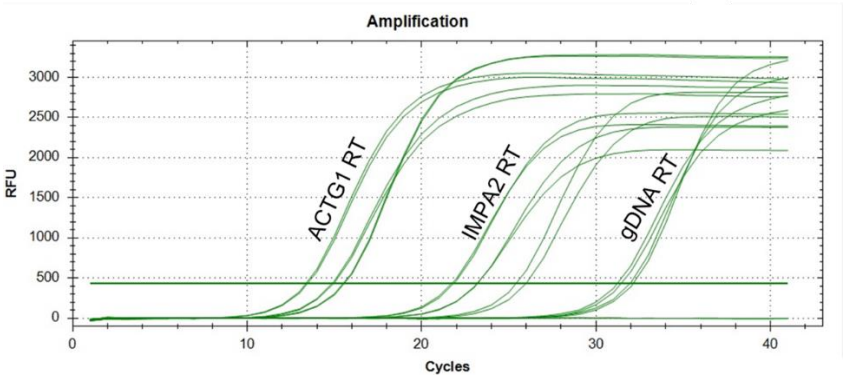

Figure 10: ***Amplification curves****: The amplification curves of ACTG1, IMPA2 and gDNA RT-qPCR reaction wells show the thresh hold cycle (Ct) for each primer assay.*

i. Genomic DNA Contamination Quantification

Genomic DNA present, and potentially amplified, during qPCR may contribute to SYBR Green reaction signals. This begs the question of how much of the total reaction signal reflects the target sequence. Relative genomic contamination was determined to be negligible using the gDNA Contamination Control Assay provided by Bio-Rad. A gDNA C_T values > 35 indicates below single copy detection (no gDNA present). For gDNA C_T values < 35, the following formula, | (GOI C_T) – (gDNA C_T) | = Δ Cq, determines the relative contribution of gDNA to the sample signal. Each Δ C_T value corresponds with a percent genomic contribution to the sample signal. For this study, any genomic contamination < 12.5% genomic contribution was considered negligible.

ii. Melt Curve Analysis Results

According to the melt curve analysis (figure 11) performed at the end of the qPCR, the melt peaks were approximately: *ISYNA1* - 88 Tm C°, *IMPA2* - 84.5 Tm C°, and ACTG1 - 85 Tm C° According to primer assay validation reports, each amplicon Tm C° was: *ISYNA1* = 88, *IMPA2* = 84.5, *ACTG1* = 85.5. Because the melt curve analysis closely matched the expected Tm, it is likely that each primer assay amplicon was the expected length. The lack of melt peaks below 80 Tm C° in the melt curve analysis showed no primer dimers contributed to qPCR signals.

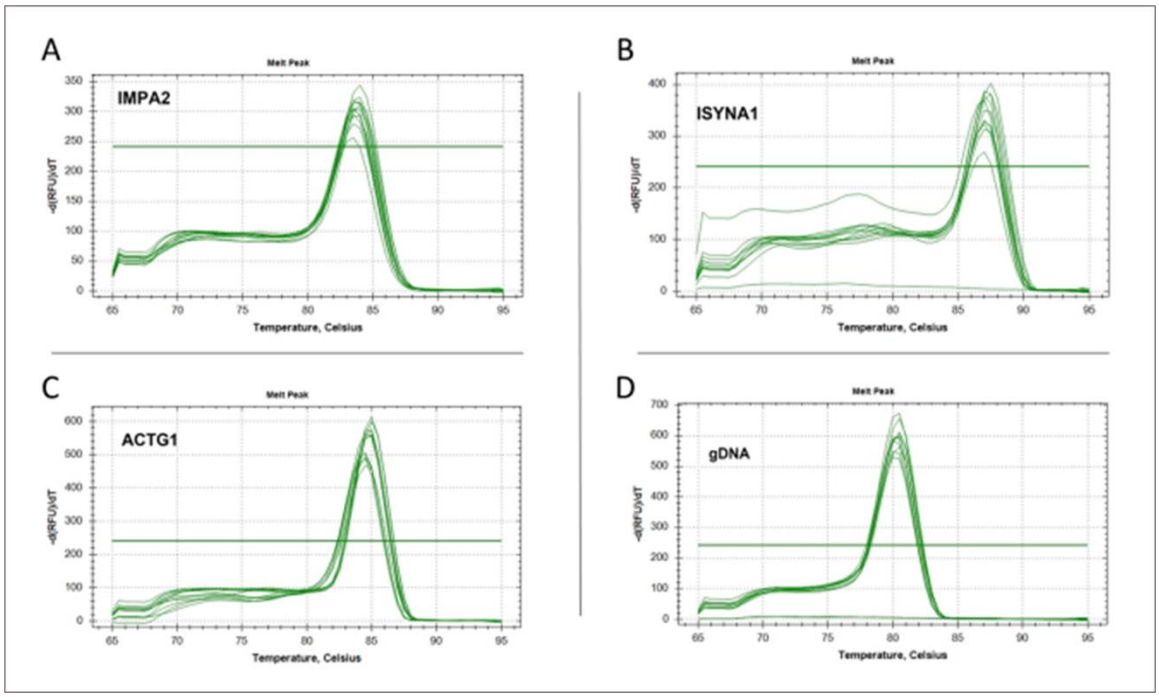

Figure 11: ***Melt Curve Analysis****: melt peaks for each primer assay were (A) IMPA2 = 84.5 Tm C° , (B) ISYNA1 = 88 Tm C°, (C) ACTG1= 85 Tm C° and (D) gDNA = 81 Tm C°.*

iii. Gel Electrophoresis Results

The results of running representative samples of each primer assay on a 5% agarose gel stained with EtBr also supported the expected product was obtained. Figure 12 shows, from left to right, the two control templates (CT); gDNA from a no RT well & RT well; and a sample from ACTG1, *IMPA2*, and *ISYNA1* RT wells. The two CT and the *IMPA2* amplicons are between 50 and 75 base pairs; the gDNA amplicons and the *ISYNA1* amplicons are close to 150 base pairs; and the ACTG1 amplicon is close to 200 base pairs. As evident by the location of the bands in the gel in figure 13, the cDNA samples and commercial templates amplified were the expected amplicon lengths.

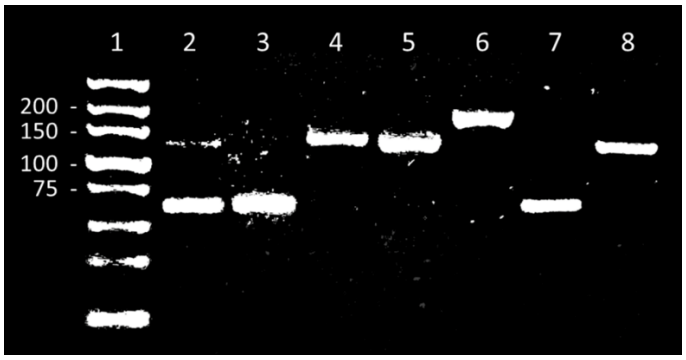

Figure 12: ***5% agarose gel dyed with EtBr.*** *From left, well 1: Ladder 300-10 bp; well 2: ISYNA1 CT; well 3: IMPA2 CT; well 4: gDNA from bipolar 2 no RT; well 5: gDNA from bipolar 2 RT; well 6: ACTG1 of bipolar 1 RT; well 7: IMPA2 of BD2 RT well 8: ISYNA1 of BD2 RT.*

The results of the genomic contamination control assay (gDNA), melt curve analysis, and 5% agarose gel validate that the sample signal C_T values represent the target amplicons. The genomic contamination control assay did detect some genomic contamination contributing to sample signals, which was considered negligible. The melt curve analysis showed no evidence of primer dimers and confirmed the amplicons for each primer assay were the expected length. The clear banding pattern in the 5% agarose gel shows each amplicon at its expected length. The results

of the genomic contamination control assay, melt curve analysis, and 5% agarose gel, validate the sample signals C_T values.

The major objective of this study was to measure possible differences in *myo*-inositol concentration and *ISYNA1* and *IMPA2* gene expression between each type of bipolar compared to healthy control. The relative gene expression of ISYNA1 was found to be 0.47-fold (bipolar 2) and 0.76-fold (bipolar 1) higher compared to non-bipolar control. The relative gene expression of IMPA2 was 2-fold (bipolar 2) and 2.1-fold higher compared to non-bipolar control. The concentration of *myo*-inositol was 13.5 g/100g in non-bipolar, 14.5 g/100g in bipolar 2, and 48.2 g/100g.

CHAPTER 4: DISCUSSION

Measuring possible differences in *myo*-inositol concentration and *ISYNA1* and *IMPA2* gene expression between each type of bipolar disorder compared to neurotypical were the major objectives of this study. The results of this study show both *ISYNA1* and *IMPA2* are expressed relatively higher in bipolar disorder, further their expression is even higher in bipolar type 1 compared to type 2. Simultaneously, the *myo*-inositol concentration is significantly higher in type 1 compared to type 2 and non-bipolar disorder. This is one of the first studies to measure relative differences in *myo*-inositol concentration and gene expression between the different types of bipolar. This and previous studies from a broader body of literature demonstrate differences associated with bipolar at the genetic, molecular, cellular, and neural circuitry levels. A population study comparing the expression of these genes between different types of bipolar could shed light on how the expression of these genes contribute to the severity of bipolar symptoms.

The focus of this study was to see if bipolar disorder patients express *IMPA2* & *ISYNA1* differently and have different *myo*-inositol concentration levels. This study found both *ISYNA1* and *IMPA2* expressed relatively higher in bipolar compared to non-bipolar; and bipolar type 1 had significantly higher concentrations of *myo*-inositol compared to type 2 and non-bipolar disorder. Not only were both genes expressed higher in bipolar compared to non-bipolar, but each gene was also expressed slightly higher in bipolar type 1 and 2. Interestingly, the results showed the expression of *IMPA2* was more than twice as high as *ISYNA1* in both types of bipolar compared to non-bipolar. The concentration of *myo*-inositol in bipolar1 was significantly higher than either type 2 or non-bipolar disorder.

These results support the hypothesis that increased available *myo*-inositol maybe directly contributing to bipolar symptoms. The relatively higher expression of *IMPA2* and ISYNA1 in both types of bipolar compared to non-bipolar supports this hypothesis because more Impase2 and MIPs

could be making more *myo*-inositol available to the cell to use in the PIP_2 network. Similarly, a postmortem study found frontal brain region *IMPA1* expression levels were not different, but *IMPA2* transcription was significantly upregulated in bipolar compared to non-bipolar (Ohnishi et al., 2007b). However, a different study measuring relative gene expression in lymphoblasts exhibiting high calcium ion levels in bipolar compared to healthy control found lower *IMPA2* expression in the type 1 cells (Yoon et al., 2001). Another study also found IMPase (not specifically IMPA1 or IMPA2) mRNA was downregulated in bipolar lymphoblasts and Lithium responders had even lower expression (Agam et al., 2009). Expression of *IMPA2* in bipolar requires more attention considering the conflicting results of this and previous studies. Additional studies comparing the expression of *IMPA1* to *IMPA2* specifically will provide a clearer understanding of each gene's involvement. Relative gene expression of *IMPA2* studies, using large population sizes, could provide clarifying results.

It would be interesting to compare how the cells regulate the expression of either *ISYNA1* and/or *IMPA2* in response to Lithium and/or VPA treatment in a larger population study. Previous studies have demonstrated Lithium and VPA interactions with MIP1 (*ISYNA1*) and IMPA1, and their fungal counterparts (Murray and Greenberg, 2000); (Dimitrova et al., 2005). This study did not consider what phase the lymphoblast donors were in nor what treatments they were on at the time of donation. Measuring differences in *myo*-inositol concentration and *ISYNA1* & *IMPA2* gene expression between the manic and depressive phases will help us fine tune treatment methods for each phase of the disorder.

The observed statistically significant difference in *myo*-inositol concentration in bipolar type 1 compared to type 2 and non-bipolar may also correlate with the more extreme symptoms of the in type 1 bipolar disorder. The results of this and previous studies suggest that the availability of *myo*-inositol may contribute to the severity of the symptoms of bipolar (Vaden et al., 2001). Additionally, studies have found reduced inositol levels in the brain of suicide victims and bipolar

patients (Shimon et al., 1997). During clinical trials, bipolar patients who were treated with inositol saw improvements in depressive symptoms (Chengappa et al., 2000). After all, the longer and more intense phases of bipolar type 1 is what differentiates type 1 from type 2 bipolar disorder (Association, 2000).

A future comparison study of individuals during the different phases of bipolar disorder could provide a clearer picture. It would be interesting to find out if cells change the expression of either *ISYNA1* or *IMPA2* in response to changes in *myo*-inositol concentration. The results of these studies may provide insight into biochemical differences between the two phases of bipolar. This may provide a basis for personalized treatment specific to the manic phase or the depressive phase.

The existing evidence points to several intracellular factors all of which affect the white matter connecting the prefrontal cortex and limbic system (Phillips et al., 2008). As stated previously, bipolar is a multi-genic disorder with several genes contributing in subtle yet critical ways to the pathophysiology of the disorder. IMPase and MIPs are not the only enzymes involved in *myo*-inositol synthesis (Harwood, 2004). Conducting future studies on each enzyme (and respective gene) related to *myo*-inositol metabolism is crucial to creating a more comprehensive picture of the PIP_2 intracellular pathway and its relationship with bipolar disorder.

Furthermore, evidence indicates genes related to oligodendrocytes and myelin appear to be abnormally expressed in schizophrenia and bipolar (Mahon et al., 2010). One study found the expression of 26 genes involved in apoptosis signaling pathways were modulated by Lithium therapy (Fries et al., 2017). Several studies have observed a variety of genetic differences between Lithium responders and non-responders (Walss-Bass and Fries, 2018). Due to *myo*-inositol's integral role in maintaining cell integrity of white matter tracts connecting the frontal lobe and limbic system, abnormalities in genes responsible for making *myo*-inositol may be contributing to bipolar.

Shedding light on *myo*-inositol's integral role in maintaining cell integrity of white matter tracts connecting the frontal lobe and limbic system, and possible abnormalities in genes responsible for making *myo*-inositol can provide novel therapeutic targets for bipolar disorder. Elucidating possible genetic differences unique to bipolar may help us better understand bipolar pathophysiology which helps improve the treatment of bipolar disorder. It would be interesting to further investigate the potential causes for the observed higher mRNA expression of *ISYNA1* and *IMPA2* in bipolar.

APPENDIX

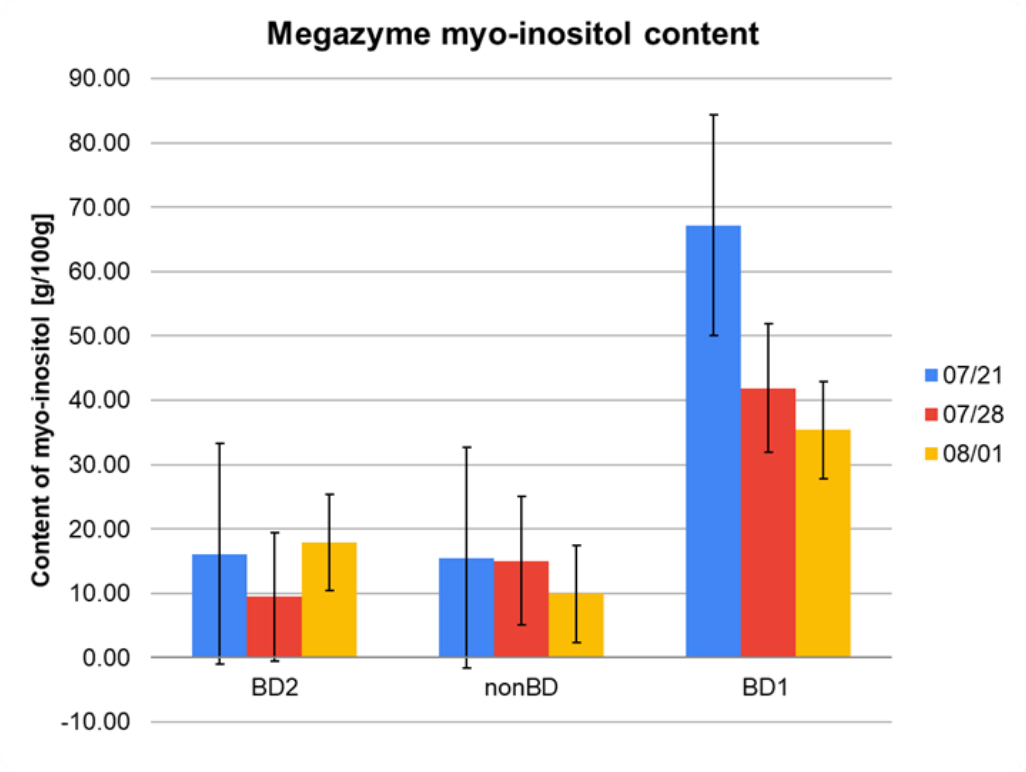

Figure 13: myo-inositol concentration graph for each of the three myo-inositol assays

A: Each of the myo-inositol concentration assay results

content of *myo*-inositol [g/100g]			
	bipolar disorder1	bipolar disorder2	non-bipolar disorder
A	67.18	16.11	15.52
B	41.89	9.48	15.04
C	35.4	17.92	9.93
Mean	48.16	14.5	13.5

Prime PCR Assay Info (from Validation Reports)					
	Amplicon length (Bipolar)	assay design	cDNA Cq	gDNA Cq	cDNA Tm (C)
ISYNA1	131	exonic	21.17	26.37	88
IMPA2	64	exonic	21.11	25	84.5
ACTG1	191	N/A	14.02	20.54	85.5
gDNA	60				

Validation Cq values based on threshold at 300 RFU

All commercial templates are synthetic DNA, length = 60 bp

Converting ΔCq to % genomic contribution

Δ Cq	% Contribution	
1	50	
2	25	
3	12.50	
4	6.25	*considered negligable*
5	3.13	
6	1.56	
7	0.78	

Figure 14: Genomic Contamination Determination Table (provided by Bio-Rad)

(PrimePCR ™ Assays, Panels, and Controls for Real-Time PCR Instruction Manual pg. 21)

REFERENCES

AGAM, G., BERSUDSKY, Y. & BELMAKER, R. H. 2009. Abnormalities of Inositol Metabolism in Lymphocytes as Biomarkers for Bipolar Disorder. *In:* RITSNER, M. S. (ed.) *The Handbook of Neuropsychiatric Biomarkers, Endophenotypes and Genes: Metabolic and Peripheral Biomarkers.* Dordrecht: Springer Netherlands.

ASSOCIATION, A. P. 2000. Bipolar Disorder (DSM-IV-TR #296.0–296.89) *Diagnostic and statistical manual of mental disorders.* 4rth Edition text revised ed. Washington, DC.

BRONSON, S. E. & KONRADI, C. 2010. Chapter 26 - Second-Messenger Cascades. *In:* STEINER, H. & TSENG, K. Y. (eds.) *Handbook of Behavioral Neuroscience.* Elsevier.

CENDRA, A., M., B. K., XIAOQIAO, X. A., FRANCOIS, F., L., R. B. & D., M. K. 2013. Modulation of the autonomic nervous system and behaviour by acute glial cell Gq protein-coupled receptor activation in vivo. *The Journal of Physiology,* 591**,** 5599-5609.

CHENGAPPA, K. R., LEVINE, J., GERSHON, S., MALLINGER, A. G., HARDAN, A., VAGNUCCI, A., POLLOCK, B., LUTHER, J., BUTTENFIELD, J., VERFAILLE, S. & KUPFER, D. J. 2000. Inositol as an add-on treatment for bipolar depression. *Bipolar Disorders,* 2**,** 47-55.

COYLE, J. T. & DUMAN, R. S. 2003. Finding the Intracellular Signaling Pathways Affected by Mood Disorder Treatment. *Neuron,* 38**,** 157-160.

DIMITROVA, A., MILANOVA, V., KRASTEV, S., NIKOLOV, I., TONCHEVA, D., OWEN, M. J. & KIROV, G. 2005. Association study of myo-inositol monophosphatase 2 (IMPA2) polymorphisms with bipolar affective disorder and response to lithium treatment. *Pharmacogenomics Journal,* 5**,** 35-41.

DIXON, J. F. & HOKIN, L. E. 1997. The antibipolar drug valproate mimics lithium in stimulating glutamate release and inositol 1,4,5-trisphosphate accumulation in brain cortex slices but not accumulation of inositol monophosphates and bisphosphates. *Proc Natl Acad Sci U S A,* 94**,** 4757-60.

FRIES, G. R., COLPO, G. D., MONROY-JARAMILLO, N., ZHAO, J., ZHAO, Z., ARNOLD, J. G., BOWDEN, C. L. & WALSS-BASS, C. 2017. Distinct lithium-induced gene expression effects in lymphoblastoid cell lines from patients with bipolar disorder. *European Neuropsychopharmacology,* 27**,** 1110-1119.

GHADIRI, M., NOURMOHAMMADI, I., FASIHI RAMANDI, M. & MOAZEN ZADEH, E. 2016. Association involving serotonin transporter gene linked polymorphic region and bipolar disorder type 1 in Iranian population. *Asia-Pacific Psychiatry,* 8**,** 92-97.

GOODWIN, F. K. & JAMISON, K. R. 2007. *Manic-Depressive Illness: Bipolar Disorders and Recurrent Depression,* New York, OXFORD University Press.

HARWOOD, A. J. 2004. Lithium and bipolar mood disorder: the inositol-depletion hypothesis revisited. *Molecular Psychiatry,* 10**,** 117.

JU, S., SHALTIEL, G., SHAMIR, A., AGAM, G. & GREENBERG, M. L. 2004. Human 1-D-myo-Inositol-3-phosphate Synthase Is Functional in Yeast. *Journal of Biological Chemistry,* 279**,** 21759-21765.

MACHADO-VIEIRA, R., MANJI, H. K. & ZARATE, C. A., JR. 2009. The role of lithium in the treatment of bipolar disorder: convergent evidence for neurotrophic effects as a unifying hypothesis. *Bipolar Disord,* 11 Suppl 2**,** 92-109.

MAHON, K., BURDICK, K. E. & SZESZKO, P. R. 2010. A role for white matter abnormalities in the pathophysiology of bipolar disorder. *Neuroscience and biobehavioral reviews,* 34**,** 533-554.

MILANESI, E., VOINSKY, I., HADAR, A., MAJ, C., KELSOE, J. R., SHEKHTMAN, T., ZANDI, P., GOES, F., POTASH, J. B., GRESHOVITS, M., GILAD, S., GENNARELLI, M., SCHULZE, T. G. & GURWITZ, D. 2017. M37 - RNA-Sequencing of Bipolar

Disorder Patients Lymphoblastoid Cell Lines Implicates A Novel Neurotrophic Factor In The Efficacy of Lithium As Mood Stabilizing Drug. *European Neuropsychopharmacology,* 27**,** S391-S392.

MURRAY, M. & GREENBERG, M. L. 2000. Expression of yeast INM1 encoding inositol monophosphatase is regulated by inositol, carbon source and growth stage and is decreased by lithium and valproate. *Molecular Microbiology,* 36**,** 651-661.

OHNISHI, T., OHBA, H., SEO, K. C., IM, J., SATO, Y., IWAYAMA, Y., FURUICHI, T., CHUNG, S. K. & YOSHIKAWA, T. 2007a. Spatial expression patterns and biochemical properties distinguish a second myo-inositol monophosphatase IMPA2 from IMPA1. *J Biol Chem,* 282**,** 637-46.

OHNISHI, T., YAMADA, K., OHBA, H., IWAYAMA, Y., TOYOTA, T., HATTORI, E., INADA, T., KUNUGI, H., TATSUMI, M., OZAKI, N., IWATA, N., SAKAMOTO, K., IIJIMA, Y., IWATA, Y., TSUCHIYA, K. J., SUGIHARA, G., NANKO, S., OSUMI, N., DETERA-WADLEIGH, S. D., KATO, T. & YOSHIKAWA, T. 2007b. A Promoter Haplotype of the Inositol Monophosphatase 2 Gene (IMPA2) at 18p11.2 Confers a Possible Risk for Bipolar Disorder by Enhancing Transcription. *Neuropsychopharmacology,* 32**,** 1727-1737.

PHILLIPS, M. L., LADOUCEUR, C. D. & DREVETS, W. C. 2008. A neural model of voluntary and automatic emotion regulation: implications for understanding the pathophysiology and neurodevelopment of bipolar disorder. *Molecular Psychiatry,* 13**,** 833-857.

RAJMOHAN, V. & MOHANDAS, E. 2007. The limbic system. *Indian Journal of Psychiatry,* 49**,** 132-139.

REGENOLD, W. T., PHATAK, P., MARANO, C. M., GEARHART, L., VIENS, C. H. & HISLEY, K. C. 2007. Myelin staining of deep white matter in the dorsolateral prefrontal cortex in schizophrenia, bipolar disorder, and unipolar major depression. *Psychiatry Res,* 151**,** 179-88.

SHIMON, H., AGAM, G., BELMAKER, R. H., HYDE, T. M. & KLEINMAN, J. E. 1997. Reduced Frontal Cortex Inositol Levels in Postmortem Brain of Suicide Victims and Patietns With Bipolar Disorder. *American Journal of Psychiatry,* 154**,** 1148 -1150.

SJØHOLT, G., GULBRANDSEN, A. K., LØVLIE, R., BERLE, J. Ø., MOLVEN, A. & STEEN, V. M. 2000. A human myo-inositol monophosphatase gene (IMPA2) localized in a putative susceptibility region for bipolar disorder on chromosome 18p11.2: genomic structure and polymorphism screening in manic-depressive patients. *Molecular Psychiatry,* 5**,** 172.

STOLL, A. L., LOCKE, C. A., MARANGELL, L. B. & SEVERUS, W. E. 1999. Omega-3 fatty acids and bipolar disorder: a review. *Prostaglandins, Leukotrienes and Essential Fatty Acids***,** 329-337.

STRECK, E. L., GONÇALVES, C. L., FURLANETTO, C. B., SCAINI, G., DAL-PIZZOL, F. & QUEVEDO, J. 2014. Mitochondria and the central nervous system: searching for a pathophysiological basis of psychiatric disorders. *Braz J Psychiatry,* 36**,** 156-67.

VADEN, D. L., DING, D., PETERSON, B. & L., G. M. 2001. Lithium and Valproate Decrease Inositol Mass and Increase Expression of the Yeast INO1 and INO2Genes for Inositol Biosynthesis. *Journal of Biological Chemistry,* 276**,** 15466–15471.

VERSACE, A., ALMEIDA, J. R., HASSEL, S., WALSH, N. D., NOVELLI, M., KLEIN, C. R., KUPFER, D. J. & PHILLIPS, M. L. 2008. Elevated left and reduced right orbitomedial prefrontal fractional anisotropy in adults with bipolar disorder revealed by tract-based spatial statistics. *Arch Gen Psychiatry,* 65**,** 1041-52.

VIDEBECH, P. 1997. MRI findings in patients with affective disorder: a meta-analysis. *Acta Psychiatrica Scandinavica,* 96**,** 157-168.

WALSS-BASS, C. & FRIES, G. R. 2018. *Are lithium effects dependent on genetic/epigenetic architecture?*

YOON, I. S., LI, P. P., SIU, K. P., KENNEDY, J. L., COOKE, R. G., PARIKH, S. V. & WARSH, J. J. 2001. Altered IMPA2 gene expression and calcium homeostasis in bipolar disorder. *Molecular Psychiatry,* 6**,** 678.

YORK, J. D., PONDER, J. W. & MAJERUS, P. W. 1995. Definition of a metal-dependent/Li(+)-inhibited phosphomonoesterase protein family based upon a conserved three-dimensional core structure. *Proc Natl Acad Sci U S A,* 92**,** 5149-53.

YU, W., DANIEL, J., MEHTA, D., MADDIPATI, K. R. & GREENBERG, M. L. 2017. MCK1 is a novel regulator of myo-inositol phosphate synthase (MIPS) that is required for inhibition of inositol synthesis by the mood stabilizer valproate. *PLoS ONE,* 12**,** 1-12.

ZHANG, S., WANG, Y., DENG, F., ZHONG, S., CHEN, L., LUO, X., QIU, S., CHEN, P., CHEN, G., HU, H., LAI, S., HUANG, H., JIA, Y., HUANG, L. & HUANG, R. 2018. Disruption of superficial white matter in the emotion regulation network in bipolar disorder. *Neuroimage Clin,* 20**,** 875-882.